# Detecting unstable periodic orbits in chaotic continuous-time dynamical systems

Detlef Pingel* and Peter Schmelcher†
*Theoretical Chemistry, Institute for Physical Chemistry, Im Neuenheimer Feld 229, University of Heidelberg, 69120 Heidelberg, Germany*

Fotis K. Diakonos‡
*Department of Physics, University of Athens, GR-15771 Athens, Greece*
(Received 19 April 2001; published 19 July 2001)

We extend the recently developed method for detecting unstable periodic points of chaotic time-discrete dynamical systems to find unstable periodic orbits in time-continuous systems, given by a set of ordinary differential equations. This is achieved by the reduction of the continuous flow to a Poincaré map which is then searched for periodic points. The algorithm has global convergence properties and needs no *a priori* knowledge of the system. It works well for both dissipative and Hamiltonian dynamical systems which is demonstrated by exploring the Lorenz system and the hydrogen atom in a strong magnetic field. The advantages and general features of the approach are discussed in detail.

DOI: 10.1103/PhysRevE.64.026214 PACS number(s): 05.45.−a

## I. INTRODUCTION

Chaotic dynamics is an intrinsic feature of many physical systems. In recent years the general importance of invariant structures in phase space for the understanding of the complex chaotic dynamics has become evident. The latter is generic in atoms and molecules but also for many other interacting and also dissipative systems. A key development of the last years to describe chaotic systems is periodic orbit theory [1–6]. It provides an expansion of the relevant properties of the system in terms of its unstable periodic orbits (UPOs) and can be applied to both classical dissipative [4–6] and Hamiltonian quantum systems [2,3]. For Hamiltonian systems, one major focus is the semiclassical energy level density. In the case of dissipative systems one is interested in properties of chaotic attractors like Lyapunov exponents, entropies and fractal dimensions, both for low-dimensional model systems [7,8] as well as for experimental time series [9–12]. Various cycle expansion techniques have been invented. The series expansions in terms of periodic orbits are usually ordered with respect to the length of the orbits [4,5,7,13,14] and converge nicely if the symbolic dynamics is well understood [4,5,15]. Additionally, periodic orbits of chaotic dynamical systems have been shown to be of great importance in order to control the corresponding systems (see Ref. [16] and references therein).

The reason why the periodic orbits of a dynamical system are not easily detectable is their instability: trajectories neighboring an UPO are repelled from it. As periodic orbits open a door to the understanding of the chaotic dynamics, many efforts have been made to develop methods to detect these orbits despite their instability from both time series or from some given set of equations of motions [8,13,15,17–19]. O. Biham and Wenzel introduced a method to compute the periodic orbits of a special class of systems up to arbitrary accuracy [19]. This approach was first applied to the Hénon map [20], and later to certain other discrete chaotic dynamical systems [14,21,22]. Several other methods have been developed to detect UPOs. However, they require a more or less accurate guess of, e.g., the initial conditions for the system under investigation. The Newton–Raphson algorithm, e.g., is a super exponential converging method to find roots, i.e., the fixed points of a map. However its starting point has to be placed in the immediate neighborhood of an existing root in order to converge and consequently find the UPO. This makes it extremely difficult to find UPOs with larger periods or to detect them for higher dimensional systems. Moreover, not all roots can be found using the Newton method. Zoldi and Greenside proposed a damped Newton method [18] that allows a less restrictive choice of the initial guess. However, for an $N$ dimensional system, each iteration step of the damped Newton method requires $O(N^3)$ operations (calculation of the stability matrix and the solution of a system of equations). It is therefore strongly desirable to have an approach that does not need extensive adaption of the initial conditions, which in turn means that no prior knowledge of specific properties of the system is necessary and/or available.

Recently, a method has been developed by two of the authors to detect periodic orbits of chaotic maps [23,24]. It has global convergence properties and needs only very marginal knowledge of the system under examination i.e., essentially only the phase space of the system. The central subject of the present investigation is the extension of this method from maps to continuous-time dynamical systems. It is organized as follows: In order to be self-contained Sec. II gives a brief outline of the method developed in Refs. [23,24] to detect periodic orbits in time-discrete systems (in the following referred to as the SD method). Sec. III is devoted to the extension of the SD method to time-continuous systems. Sections IV and V contain applications to two continuous–time dynamical systems: the dissipative Lorenz system and the conservative Hamiltonian system describing the hydrogen atom in a strong magnetic field. Section VI provides a summary of the essentials and gives an outlook on possible future investigations.

*Email address: detlef.pingel@tc.pci.uni-heidelberg.de
†Email address: peter.schmelcher@tc.pci.uni-heidelberg.de
‡Email address: fdiakono@cc.uoa.gr

 

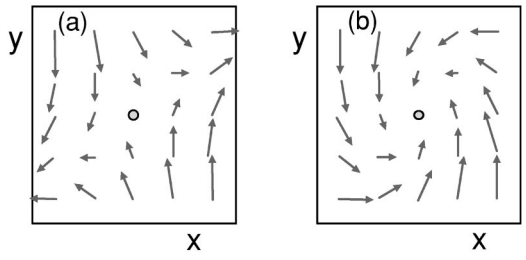


FIG. 1. (a) Vector field around a saddle point; (b) stabilization is achieved by inverting the sign of the $x$ component of the flux vectors.

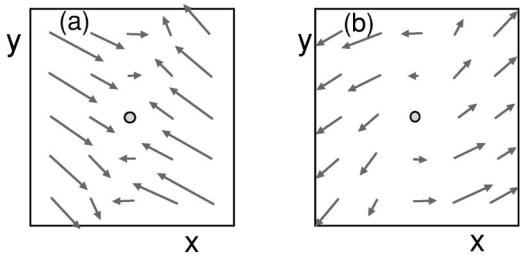


FIG. 2. (a) Vector field around a saddle point different from Fig. 1; (b) inverting the sign of the $x$ component of the flux vectors does not yield stabilization.

## II. DETECTING PERIODIC ORBITS IN TIME–DISCRETE CHAOTIC SYSTEMS

In Refs. [23–25] a set of special transformations is invented in order to transform a dynamical system such that the following properties hold. The positions of the UPOs in phase space are the same for the original chaotic system and the transformed dynamical systems but their stability properties have changed: unstable fixed points turned into dissipatively stable ones. A trajectory of the transformed system starting in the domain of attraction of a stabilized fixed point converges in it. The UPOs of a chaotic dynamical system can therefore be obtained by iterating the transformed systems using a (robust) set of initial conditions.

To substantiate the above ideas we start with a given time-discrete dynamical system, i.e., a map $\mathbf{f}$:

$$\mathbf{x}_{i+1}=\mathbf{f}(\mathbf{x}_i) \tag{1}$$

Our goal is to find the UPOs of length $p$ of the map $\mathbf{f}$, i.e., the fixed points $\mathbf{x}_o$ of the $p$ times iterated map $\mathbf{f}^{(p)}$

$$\mathbf{x}_o=\mathbf{f}^{(p)}(\mathbf{x}_o). \tag{2}$$

To this aim, let us define a flux vector $\mathbf{F}(\mathbf{x})$,

$$\mathbf{F}(\mathbf{x})=\mathbf{f}^{(p)}(\mathbf{x})-\mathbf{x}. \tag{3}$$

Clearly the position of the fixed points of the map $\mathbf{f}^{(p)}$ and the stationary points of the flow $\dot{\mathbf{x}}=\mathbf{F}(\mathbf{x})$ defined by $\mathbf{F}$ are the same. The transformations of the SD method are of global geometrical character in the sense that they contain, e.g., an exchange or a reverse of the sign of certain components occurring in the above flux vector $\mathbf{F}$. In the course of these transformations the flux vectors of the original system around a stationary point become focused towards this point. Figure 1 provides an example of a stabilizing transformation that consists of reversing the sign of the $x$ component of $\mathbf{F}(\mathbf{x})$. The set of fixed points of $\mathbf{f}^{(p)}$ cannot be expected to be stabilized by just one particular transformation. Figure 2(a), for example, shows a fixed point different from the one depicted in Fig. 1(a) for which the transformation applied in Fig. 1 does not yield the desired stability [see Fig. 2(b)]. Therefore, a complete set of transformations is necessary in order to render all UPOs stable. These transformations are linear with respect to the flux vector $\mathbf{F}(\mathbf{x})$. The corresponding matrices have only one nonvanishing entry $+1$ or $-1$ in each row and column, i.e., they are orthogonal. In two dimensions, the complete set of matrices are as follows:

$$\mathbf{C}_1=\begin{pmatrix}1&0\\0&1\end{pmatrix},\quad \mathbf{C}_2=\begin{pmatrix}-1&0\\0&-1\end{pmatrix},\quad \mathbf{C}_3=\begin{pmatrix}-1&0\\0&1\end{pmatrix},$$

$$\mathbf{C}_4=\begin{pmatrix}1&0\\0&-1\end{pmatrix}, \tag{4}$$

$$\mathbf{C}_5=\begin{pmatrix}0&1\\-1&0\end{pmatrix},\quad \mathbf{C}_6=\begin{pmatrix}0&-1\\1&0\end{pmatrix},\quad \mathbf{C}_7=\begin{pmatrix}0&-1\\-1&0\end{pmatrix},$$

$$\mathbf{C}_8=\begin{pmatrix}0&1\\1&0\end{pmatrix} \tag{5}$$

and the transformed systems evolve according to

$$\mathbf{S}_k:\quad \dot{\mathbf{x}}=\mathbf{S}_k(\mathbf{x})=\mathbf{C}_k\mathbf{F}(\mathbf{x})=\mathbf{C}_k[\mathbf{f}^{(p)}(\mathbf{x})-\mathbf{x}],\qquad k=1,\ldots,8. \tag{6}$$

It can be shown that any given fixed point of a fully chaotic two-dimensional system is stable in exactly two of the eight systems $\mathbf{S}_k$ [23–25]. Therefore, propagating a (sufficient) set of starting points with each of the eight systems and looking for the stationary points to which the trajectories converge will yield the complete set of fixed points of $\mathbf{f}^{(p)}$. The differential equations (6) can be integrated using a standard numerical integration routine. However, for reasons of simplicity we prefer to go back to discrete time and discretize the equations of motion (6) via the Euler discretization

$$\dot{\mathbf{x}}\rightarrow(\mathbf{x}_{i+1}-\mathbf{x}_i)/\lambda, \tag{7}$$

with a small time step $\lambda$. This yields the following discrete transformed systems:

$$\tilde{\mathbf{S}}_k:\quad \mathbf{x}_{i+1}=\mathbf{x}_i+\lambda\mathbf{C}_k[\mathbf{f}^{(p)}(\mathbf{x}_i)-\mathbf{x}_i]. \tag{8}$$

The implementation of the equation (8) is straightforward and no integration routine is needed. Numerically, it turns out that the basin of attraction of a periodic point that is stable in one of the SD-transformed systems is not restricted to the linear neighborhood of the fixed point, as it is the case of the Newton method. It has a global geometrical extension and covers a comparatively large area of the phase space of the system. Trajectories that start at a large distance from the periodic point approach its linear neighborhood rapidly. This

is an essential advantage compared to the Newton method. The Newton algorithm needs both the initial point to be close to the fixed point and needs the evaluation of the stability matrix for each step. What is more, only roots $\mathbf{x}_o$ of a function $f$ with $|f''f/(f')^2|<1$ and be found with the Newton method. These requirements are not necessary when applying the SD method. This makes the SD method a powerful tool to find UPOs in time-discrete maps. It generally suffices to propagate a set of initial points with a minimal set of stabilizing SD transformations. For fully chaotic dynamical systems (i.e., there is no repeller with unstable directions only) the minimal sets are proven to be [25]

$$\{\mathbf{C}_1,\mathbf{C}_3,\mathbf{C}_4\} \qquad \text{or} \qquad \{\mathbf{C}_1,\mathbf{C}_7,\mathbf{C}_8\}. \tag{9}$$

The set of starting points are best taken from the attractor in case of dissipative systems (UPOs are dense in the chaotic attractor) or uniformly distributed in phase space for area-preserving maps. The trajectories of the transformed systems $\tilde{\mathbf{S}}_k$, starting from these initial points, converge in those periodic points that are stable in $\tilde{\mathbf{S}}_k$. Having propagated the minimal set of SD-transformed systems, all that has to be done is to omit the multiple occurrence of the detected fixed points. Apart from the global convergence properties, the SD method has the advantage that it contains only a single parameter $\lambda$ that determines the step size of the transformed dynamical system and is closely related to the stability of the fixed point. The smaller $\lambda$ is, the more unstable are the fixed points that can be detected. This relation between $\lambda$ and the stability is strictly monotonous in the case of the SD transformation $\mathbf{S}_1$, while the other transformations show an at least approximate ordering [25,26]. This fact allows a detection of UPOs being selective with respect to their stability.

The SD method has been already applied successfully [23–25] to several time-discrete maps like Hénon map [20] and Ikeda map [27]. It proved to be very effective for studies of the stability properties of UPOs of two-dimensional maps [28]. Other applications include the detection of unstable high-period orbits used for control of complex systems [29], estimation of generating partitions of chaotic systems [30], and the analysis of the unstable dimension variability [31]. Recently, the convergence properties of an algorithm by Davidchack and Lai [32] that is based on the SD method has been studied [33] in detail. Also in Ref. [34] a successful attempt has been made to detect periodic orbits of higher dimensional systems using the SD method combined with a so-called subspace fixed–point iteration.

A majority of dynamical systems in physics however are continuous in time, i.e., their time evolution is described by differential equations. The extension of the SD method to time-continuous systems is the main point of this paper. We want to demonstrate the general applicability of the SD method to detect UPOs in time-continuous dissipative or Hamiltonian systems with compact phase space.

## III. DETECTING PERIODIC ORBITS IN TIME-CONTINUOUS SYSTEMS

UPOs of a given length $p$ of a map $\mathbf{f}$ are nothing but fixed points of the $p$ times iterated map $\mathbf{f}^{(p)}$. The SD-transformed systems are designed such that a relevant part of the trajectories converges to these fixed points. In principle, these ideas apply to time-continuous systems as well. If the length of the UPOs to be found would be known exactly, one would simply apply the SD method to detect them. However, in contrast to time-discrete systems the period is now a continuous quantity. Therefore a direct transfer and application of the method is not possible.

Let the original continuous (chaotic) system be given by a system of ordinary differential equations, i.e., by the flow

$$\dot{\mathbf{x}}=\mathbf{G}(\mathbf{x}). \tag{10}$$

Next we introduce a hyperplane in phase space that defines a Poincaré surface of section (PSS). The latter can be constructed by recording successive intersections of the continuous trajectories with the hyperplane in the same direction. This yields a Poincaré map $\mathbf{g}_\mathbf{G}(\mathbf{x})$ belonging to the flow $\mathbf{G}(\mathbf{x})$. UPOs of the time-continuous system correspond to periodic points of the Poincaré map, i.e., to fixed points of the correspondingly iterated Poincaré map. The intersections of a trajectory of the system with the PSS are easily obtained by integrating the flow and continuously asking for the single condition fulfilled by the hyperplane followed by an iteration procedure to specify these points. Applying the SD transformations to the Poincaré map the dynamics takes place in a $(N-1)$-dimensional subspace of the $N$-dimensional phase space. Therefore, the minimal set of stabilization transformations for dimension $N-1$ is needed only.

As already pointed out in the previous section, one major advantage of the SD method is clearly its global convergence property. This feature is equally present when the method is applied to detect UPOs in PSS of time-continuous systems. In all examples considered below, the extensions of the basins of attraction are typically many orders of magnitude larger than the corresponding linear neighborhoods. For longer orbits, these basins of attraction tend to take on a fractallike and fiberlike appearance. Another advantage of the SD method is the fact that no knowledge about the continuous dynamical system is needed. There exist a number of methods to find UPOs of chaotic dynamical systems by defining certain symbolic sequences for the dynamics of the system or by taking advantage of certain symmetries of the equations of motion. None of these considerations are necessary when dealing with the SD method. All one needs is a numerical routine to reliably integrate the equations of motion and a coarse-grained set of starting points.

Starting with a trajectory in the basin of attraction of a certain UPO, the speed of the convergence of the SD-transformed system decreases with decreasing distance of the corresponding starting point from the fixed point. In the linear neighborhood of the fixed point, the distance $d_n$ of the $n$th point of the trajectory $\{\mathbf{x}_n\}$ to the fixed point decreases exponentially like $d_{n+1}/d_n=1-\lambda\Lambda$, where $\Lambda$ is the most unstable eigenvalue of the fixed point in the original system and $\lambda$ is the parameter of the SD algorithm (usually $\lambda \ll 1/\Lambda$). Therefore the propagation speed can slow down considerably, particularly when a small value of $\lambda$ is used. In this case the algorithm may become increasingly inefficient

if a high resolution of the position of an UPO with a long period is required. The linear neighborhood of the fixed point is the regime where the well-established Newton method applies and converges superexponentially. In our investigations of time-continuous systems we therefore combine the SD-method with a Newton method. It turned out to be most efficient to interrupt the iteration of the SD-transformed system and make a trial shot with the Newton algorithm when the step length of the SD algorithm is below a given value. The Newton procedure then either does not converge at all, or it converges to a periodic point within a few (typically not more than ten) iterations. In the first case, the propagation of the SD algorithm is continued at the point where it has been stopped. In the second case, one has to check whether the Newton algorithm has converged to the same fixed point as the SD algorithm did. The latter is recommended in order to allow for a classification of the fixed points found. A fixed point that attracts a trajectory has certain geometrical features that are related to the specific transformed system that is propagated (see [25] for details). This close correlation is lost when the SD and the Newton algorithm are allowed to converge to different points. Additionally, the assignment of a basin of attraction becomes meaningless if a random element like an uncontrolled Newton process is made use of.

Let us now provide some comments on the implemented Newton algorithm (for more details see, e.g., [5]). The Jacobian matrix $\mathbf{J}$ along a trajectory obeys the equation of motion

$$\dot{\mathbf{J}}(t)=\frac{\partial \mathbf{G}(\mathbf{x})}{\partial \mathbf{x}}\mathbf{J}(t) \tag{11}$$

with the initial condition

$$\mathbf{J}(t=0)=\mathbf{1}. \tag{12}$$

The trajectory $\mathbf{x}(t)$ and the Jacobian $\mathbf{J}(t)$ can be integrated simultaneously using the same integration routine [considering the entries of $\mathbf{J}(t)$ as additional coordinates of $\mathbf{x}(t)$]. Now we propagate an initial condition $\mathbf{x}$ on the PSS to a successive intersection $\mathbf{g_G}(\mathbf{x})$, which takes the time $T(\mathbf{x})$. Linearizing around the flow yields for a point $\mathbf{x}'$ in the neighborhood of $\mathbf{x}$:

$$\mathcal{G}(\mathbf{x},\mathbf{x}')\approx \mathbf{g_G}(\mathbf{x})+\mathbf{J}(\mathbf{x}'-\mathbf{x}), \tag{13}$$

where $\mathbf{J}$ is obtained by integrating Eq. (11) between the two successive intersections at $\mathbf{x}$ and $\mathbf{g_G}(\mathbf{x})$. $\mathcal{G}(\mathbf{x},\mathbf{x}')$ describes the image of $\mathbf{x}'$ after the time $T(\mathbf{x})$. Generally, $\mathcal{G}(\mathbf{x},\mathbf{x}')$ is not on the surface, even though $\mathbf{x}$, $\mathbf{x}'$ and $\mathbf{g_G}(\mathbf{x})$ are. This is because the times required to propagate $\mathbf{x}$ and $\mathbf{x}'$, until the next intersection with the PSS, are different. To find a fixed point $\mathbf{x}_o=\mathbf{g_G}(\mathbf{x}_o)$ consider Eq. (13) as an equality and set $\mathcal{G}(\mathbf{x},\mathbf{x}')=\mathbf{x}'$. Then the following linearized equation has to be solved for $\mathbf{x}'$:

$$(\mathbf{1}-\mathbf{J})(\mathbf{x}'-\mathbf{x})=-[\mathbf{x}-\mathbf{g_G}(\mathbf{x})]. \tag{14}$$

To achieve this, two problems have to be addressed. The first one concerns the fact that $\mathbf{J}$ possesses a unit eigenvector along the flow $\mathbf{G}(\mathbf{x})$. Therefore the matrix $\mathbf{1}-\mathbf{J}$ is singular and cannot be inverted. The second problem is the fact that the solution $\mathbf{x}'$ is in general not in the PSS, as explained above. Both obstacles can be removed by adding a small vector $\mathbf{G}(\mathbf{x})\delta T$ along the flow $\mathbf{G}(\mathbf{x})$ to Eq. (14) [see Eq. (16) below]. This bends the eigenvalue of $\mathbf{J}$ away from unity. At the same time, the vector $(\mathbf{x}'-\mathbf{x})$ can be constrained to the PSS. For the systems studied, the PSS are hyperplanes in phase space, i.e., we have

$$(\mathbf{x}'-\mathbf{x})\cdot\mathbf{a}=0 \tag{15}$$

with the normal vector $\mathbf{a}$. Equation (14) now becomes

$$\begin{pmatrix}\mathbf{1}-\mathbf{J} & \mathbf{G}(\mathbf{x})\\ \mathbf{a} & 0\end{pmatrix}\begin{pmatrix}\mathbf{x}'-\mathbf{x}\\ \delta T\end{pmatrix}=\begin{pmatrix}-[\mathbf{x}-\mathbf{g_G}(\mathbf{x})]\\ 0\end{pmatrix}. \tag{16}$$

Inversion of the matrix on the left-hand side of the equation above yields the position $\mathbf{x}'$, resulting from $\mathbf{x}$ within one step of the Newton algorithm.

As discussed above, we found it most economic to combine the numerical algorithms in a way that either the SD method or the Newton procedure is applied. Nonetheless, recently a different hybrid approach has been suggested for discrete time systems, i.e., maps [32]. It combines the advantages of both methods (SD and Newton) *in each step* of the corresponding hybrid algorithm and is therefore very efficient for sufficiently low-dimensional systems. However for each step the stability matrix has to be integrated and to be inverted, which makes this hybrid approach less promising for higher-dimensional systems. Furthermore, the strong correlation of the geometrical features of the fixed point that becomes stable and the corresponding SD transformation that achieves this is, in general, reduced. One cannot be sure that the UPO the algorithm converges to is actually stable in the pure SD-transformed system.

There are three important elements of the SD method as applied to time-continuous systems: The choice of the PSS, the set of starting points, and, finally, the value of the parameter $\lambda$ that determines the step size of the propagation. These elements can be utilized as tools if one is especially interested in UPOs with certain features and will therefore be addressed in the following in more detail.

Obviously, only orbits that intersect with the PSS can be detected. The freedom in the choice of the PSS has to be considered as an advantage or more precisely as a selective tool for the detection of the UPOs. In general the appearance of the UPOs can, to a crude extent, be controlled by the choice of both the PSS and the requested number of intersections: Searching for long periods and a small number of intersections will yield orbits that are predominantly localized far from the chosen PSS, whereas the quest for relatively small periods with a large number of intersections results in orbits that are localized close to the PSS (see Sec. V). The distribution of the periods of the UPOs to be found can, to some extent, be controlled by the parameter $\lambda$ whose importance will be discussed next.

The parameter $\lambda$ [see Eq. (7)] has the meaning of an elementary time step for the SD-transformed system. On the other hand, it is also related to the stability of the UPOs that

should be detected. Let us explain why. The stability matrix of the transformed continuous systems in Eq. (6) reads

$$\mathbf{M}_{\mathbf{S}_k}(\mathbf{x}) = \mathbf{C}_k(\mathbf{M}_{\mathbf{g}^{(p)}}(\mathbf{x}) - \mathbf{1}), \tag{17}$$

where $\mathbf{M}_{\mathbf{g}^{(p)}}(\mathbf{x})$ is the stability matrix at the fixed point $\mathbf{x}$ of the $p$ times iterated Poincaré map $\mathbf{g}^{(p)}$. Let $\mathbf{M}_{\mathbf{S}_k}(\mathbf{x})$ have eigenvalues $\Lambda_i$. Fixed points in these systems are stable $\mathrm{Re}(\Lambda_i) < 0$. The discretised version of Eq. (17) belonging to Eq. (8) possesses the stability matrix

$$\mathbf{M}_{\tilde{\mathbf{S}}_k}(\mathbf{x}) = \mathbf{1} + \lambda \mathbf{C}_k(\mathbf{M}_{\mathbf{f}^{(p)}}(\mathbf{x}) - \mathbf{1}) \tag{18}$$

with eigenvalues $1 + \lambda\Lambda_i$ (the position of the fixed points of the continuous and the discrete system are the same). However, in order to be stable in the discrete system, the eigenvalues of the stability matrix $\mathbf{M}_{\tilde{\mathbf{S}}_k}(\mathbf{x})$ must have the modulus $|1 + \lambda\Lambda_i| < 1$. For highly iterated maps $\mathbf{g}^{(n)}$, $n$ large, we have the typical situation $\Lambda_i \ll -1$ and it is obvious that there exists an upper limit for $\lambda$ such that the fixed point is still stable in the transformed system [see Eq. (8)]. Therefore the parameter $\lambda$ determines the set of fixed points that can be found by the discretized algorithm (8). For example, only being interested in UPOs that are weakly unstable (e.g., for utilization in a stability-ordered cycle expansion) a relatively large value of $\lambda$ will do a good job. As a side effect the propagation time decreases (the step size is relatively large) and the domains of attraction have large extensions. The smaller the value of $\lambda$, the larger the set of detected fixed points will be.

The performance of the SD-method depends also on the set of starting points. One possibility is to sample the set of initial points from a chaotic trajectory. This will be the strategy for dissipative systems (see Sec. IV) or attractors in general (for a different approach to the selection of initial points see Ref. [32]). For chaotic ergodic Hamiltonian systems it is natural to choose a uniform distribution of initial points on the PSS. Due to the global convergence character of the SD method the set of starting points plays only a minor role compared to, e.g., the Newton method.

In the following we present two studies of continuous time dynamical systems: The three-dimensional dissipative Lorenz system and the Hamiltonian system consisting of the hydrogen atom in a strong homogeneous magnetic field, which possesses two relevant degrees of freedom. For both systems, the PSS is two-dimensional. Therefore, a minimal set of only three SD-transformations is sufficient to detect all fixed points of the Poincaré map, i.e., all UPOs of the original continuous-time system.

## IV. THE LORENZ SYSTEM

The Lorenz model [35] provides a three-dimensional model of the atmospheric convection. The corresponding equations of motion are

$$\dot{x} = \sigma y - \sigma x, \tag{19}$$

$$\dot{y} = -xz + \rho x - y, \tag{20}$$

$$\dot{z} = xy - \beta z. \tag{21}$$

In this model, the coordinates $x$, $y$, and $z$ are related to the circulatory fluid flow velocity, the temperature gradient and nonlinear deviations of the temperature profile. We considered the following values of the parameters:

$$\sigma = 16.0, \quad \beta = 4.0, \quad \varrho = 45.92. \tag{22}$$

Although the Lorenz system is originally three dimensional, rapid phase space contraction leads to an essentially two-dimensional attractor. Taking the gradient of the phase space flow, one can see that the exponential contraction rate is $(1 + \sigma + \beta)$, i.e., $V(t) = V(0)e^{-(1+\sigma+\beta)t}$ [36]. The dynamics is restricted to two nearly flat rotating plates. The centers of the rotating motion are located at the stationary points $[\pm\sqrt{\beta(\varrho-1)}, \pm\sqrt{\beta(\varrho-1)}, \varrho-1]$, and a third stationary point is at $(0,0,0)$. For use in geophysical studies the stationary points of a model system are of prominent importance. Further significant insight can be gained by analyzing the UPOs of this system, which makes it an ideal testing ground for our approach. All of these orbits are unstable. Many features of the Lorenz system, including UPOs and their bifurcations, are discussed by Sparrow [37]. Several methods have been suggested so far to detect UPOs in this system (see [36] and references therein). The Newton method works fine in principle, but requires a good guess of the initial conditions.

We now demonstrate that the SD method discussed in the previous section works extremely well for the detection of the UPOs in the Lorenz system. The PSS is given by $\{(x,y,z | z = \varrho - 1\}$. This (hyper)plane contains the two nontrivial stationary points. Since each UPO oscillates around one and/or both of these stationary points, they have to intersect with the PSS and yield therefore fixed points of the corresponding Poincaré map. Propagating the set of initial points with the various SD-transformed systems, trajectories often converge to the two stationary points contained in the PSS. This is an undesired effect and we avoided a loss of efficiency due to it by stopping the propagation of the trajectory as soon as it is close to either of the two stationary points (it might happen that this way certain periodic points of the Poincaré map are excluded from detection, but since an UPO generically possesses also points at larger distances from the stationary points, it is extremely unlikely that it is missed because of this procedure). Since the chaotic attractor of the Lorenz system is nearly two dimensional the set of intersections with the PSS is almost linear. It is therefore not favorable to sample initial points randomly from the Poincaré hyperplane (the SD algorithm would work well with these initial points, too, but the paths of convergence would be rather long). It is instead recommendable to sample points from a chaotic trajectory after a sufficient transient time has passed. It turned out to be efficient to take not a complete section of the trajectory but short random segments. The reason for this is the intermittent behavior of the trajectories that results in the same fixed points obtained for many successive starting points from a trajectory.

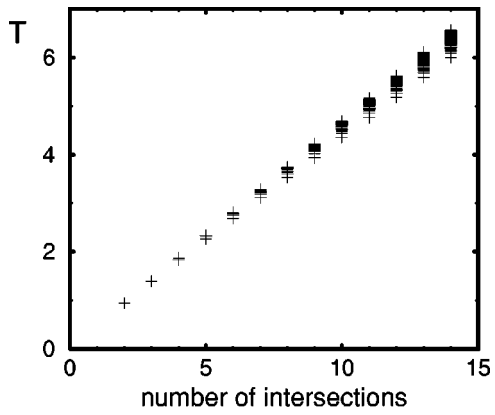


FIG. 3. The Lorenz system: Distribution of the length of the periodic orbits versus the number of their intersections with the PSS.

The λ parameter has to be adjusted each time a different number of intersections of the UPOs is required. This can be achieved by choosing the stabilization matrix $\mathbf{C}_1=\mathbf{1}$ and adjusting λ such that all or nearly all initial points converge (the stabilized system corresponding to $\mathbf{C}_1$ is likely to converge from any point in the phase space, λ being sufficiently small). For the Lorenz system the relation of the length of the UPOs to the number of their intersections with the PSS is approximately one dimensional which is illustrated in Fig. 3. The instability of the orbits generally increases with their length. Therefore, the value of λ has to be decreased if UPOs with a larger number of intersections should be detected. This relation looks very different for the hydrogen atom in a magnetic field (see next section).

As explained in the previous section, the numerical efficiency can be dramatically improved by combining the SD method with a Newton algorithm. The time to switch the propagation from one method to the other is crucial for the efficiency of the algorithm. We found the following procedure to be most effective: The trajectory is propagated with the SD algorithm, starting from some initial point, until a step size $|\mathbf{g}^{(p)}(\mathbf{x})-\mathbf{x}|<\epsilon$ is reached (typically $\epsilon=0.1$). Then it is checked whether the above defined step size decreases further while applying the SD algorithm. If not (λ is still too large to provide convergence) the SD algorithm is continued. Elsewise, i.e., if the step size is decreasing constantly the Newton algorithm is switched on. In case it converges it does so within a few ($\leqslant 10$) steps and converges close to the point where the SD algorithm was terminated. If the convergence pattern differs from the above, the fixed point of the Newton algorithm is likely to be different from the fixed point the pure SD algorithm would yield. In the latter case, the fixed point found by the Newton method is discarded, since the correlation of the detected fixed points and the corresponding SD transformations is strongly desired. The propagating scheme then switches back to the SD algorithm. Provided the parameter λ is small enough, it typically takes less than 50 steps of the SD algorithm and less than 10 steps for the Newton algorithm to determine the position of the UPOs within an accuracy of $|\mathbf{g}^{(p)}(\mathbf{x})-\mathbf{x}|\leqslant 10^{-14}$.

In Table I the numerical results for the Lorenz system are given. It provides the number of prime UPOs and their mean period, sorted with respect to the number of intersections with the PSS. Reference [36] gives the number of prime orbits for $p\leqslant 12$ that coincide with our data in Table I. The mean length of the UPOs grows approximately linear with the number of intersections of the orbit. This reflects the circular shaped dynamics of the Lorenz system: Trajectories, and therefore also UPOs, rotate around the nontrivial stationary points with nearly constant frequency. Figure 3 shows the almost linear dependence as well as the small variance of the length of the UPOs with the number of intersections. The last two rows of Table I give some numerical properties of the SD algorithm: the size of the λ parameter and the number of initial points needed to detect all UPOs. It is remarkable that this number roughly coincides with the number of detected periodic points. However, it has to be kept in mind that not all initial points converge and this set therefore, has to be slightly larger than the numbers $N_i$ given in Table I. The SD method is capable of locating UPOs with a remarkable large number of intersections. Figure 4 displays an example of an UPO with 30 intersections (in the same direction) with the PSS. It clearly exhibits the elements all orbits of the Lorenz system are composed of: The rotating motion in the two planes with a varying number of turnovers between them. Remarkably, all UPOs can be found by propagating only one of the SD-transformed systems, i.e., $\tilde{\mathbf{S}}_4$ with the matrix $\mathbf{C}_4$. Figure 5 shows the set of intersections of the UPOs given in Table I. It demonstrates clearly the nearly two-dimensional extension of the chaotic attractor. It is possible that the low dimension of the attractor is related to the fact that only one SD-transformed system $\tilde{\mathbf{S}}_4$ is sufficient to find all UPOs.

## V. THE HYDROGEN ATOM IN A STRONG MAGNETIC FIELD

The hydrogen atom in a strong homogeneous magnetic field is also known in the literature as the diamagnetic Kepler problem. With increasing degree of excitation i.e., increasing energy and/or increasing field strength its classical dynamics

TABLE I. Lorenz system. Properties of periodic orbits with 2 up to 14 intersections with the PSS, and parameters of the numerical detection: the parameter λ and the required number of converged initial points $N_i$, sampled from the attractor.

| Number of intersections | 2 | 3 | 4 | 5 | 6 | 7 | 8 | 9 | 10 | 11 | 12 | 13 | 14 |
|---|---|---|---|---|---|---|---|---|---|---|---|---|---|
| Number of prime orbits | 1 | 2 | 3 | 6 | 9 | 18 | 30 | 56 | 99 | 186 | 335 | 630 | 1160 |
| Mean period | 0.941 | 1.394 | 1.843 | 2.305 | 2.756 | 3.219 | 3.676 | 4.136 | 4.595 | 5.054 | 5.514 | 5.974 | 6.433 |
| λ | 0.1 | 0.1 | 0.1 | 0.05 | 0.01 | 0.01 | 0.001 | 0.001 | 0.001 | 0.001 | 0.0001 | 0.0001 | 0.0001 |
| $N_i$ | 1 | 3 | 11 | 17 | 144 | 40 | 192 | 687 | 1094 | 2523 | 3773 | 10498 | 11472 |

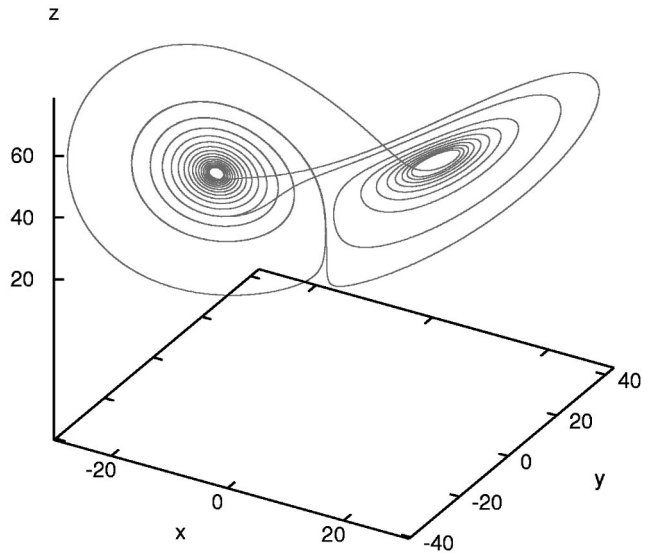


FIG. 4. The Lorenz system: An example of a long periodic orbit with 30 intersections with the PSS.

is well known to become almost completely chaotic. Unstable periodic orbits have been extensively used (see Refs. [38–41] and references therein) to semiclassically quantize this system and to obtain detailed information on a variety of properties (level density, scarring of wave functions etc.). Therefore several methods have already been developed to detect UPOs in this system by searching, e.g., along symmetry lines in configuration space [41]. Some of these methods are based on assigning a certain symbolic code to the individual UPOs and most of them are specially designed for the diamagnetic Kepler problem. As already mentioned above the SD approach needs no such prior knowledge and will be demonstrated to work very well also for this Hamiltonian system: No discussion of symmetry is needed and no symbolic code has to be developed. All what is necessary is a numerical routine to integrate the equations of motions, the proper definition of the PSS and a chaotic trajectory to sample the initial points from. We emphasize that the diamagnetic Kepler problem is just one although prominent example of a physical system that can be analyzed with help of the SD algorithm.

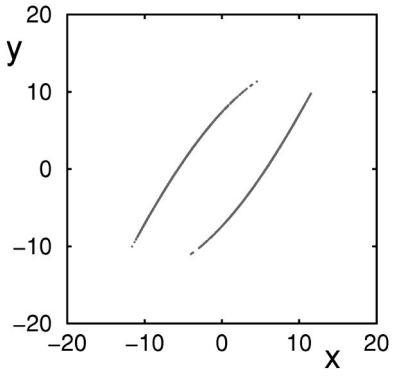


FIG. 5. The Lorenz system: The location of periodic orbits with 2 up to 14 intersections in the PSS.

The Hamiltonian of the hydrogen atom in a strong magnetic field assuming an infinite nuclear mass reads in atomic units

$$H=\frac{\mathbf{p}^2}{2}-\frac{1}{|\mathbf{r}|}+\frac{1}{2}\gamma l_z+\frac{1}{8}\gamma^2(x^2+y^2). \tag{23}$$

It depends on the relative coordinates $\mathbf{r}$ and momenta $\mathbf{p}$ of the electron with respect to the nucleus. $l_z$ represents the component of the angular momentum parallel to the magnetic field $\gamma$. Rescaling the coordinates (e.g., Ref. [38]) according to

$$\tilde{\mathbf{r}}=\gamma^{2/3}\mathbf{r} \qquad \text{and} \qquad \tilde{\mathbf{p}}=\gamma^{-1/3}\mathbf{p} \tag{24}$$

the dynamics, i.e., the Hamiltonian equations of motion depend now only on the scaled energy $\epsilon$,

$$\epsilon=\gamma^{-2/3}E \tag{25}$$

and not on $E$ and $\gamma$ separately. The singularity at $\tilde{\mathbf{r}}=0$ is a drawback of the above Hamiltonian. It can be removed e.g., by the introduction of semiparabolic coordinates (e.g., Ref. [38]):

$$\nu^2=|\tilde{\mathbf{r}}|-\tilde{z}, \qquad \mu^2=|\tilde{\mathbf{r}}|+\tilde{z}, \tag{26}$$

where the momenta

$$p_\nu=\frac{d\nu}{d\tau}, \qquad p_\mu=\frac{d\mu}{d\tau} \tag{27}$$

are defined with respect to the scaled time $\tau$ given by

$$dt=2|\tilde{\mathbf{r}}|d\tau=(\nu^2+\mu^2)d\tau. \tag{28}$$

The equations of motion generated by the Hamiltonian (23) for a fixed value of the scaled energy are equivalent to the equations of motion generated by the Hamiltonian

$$h(\mu,\nu,p_\mu,p_\nu)=\frac{p_\nu^2}{2}+\frac{l_z^2}{2\nu^2}+\frac{p_\mu^2}{2}+\frac{l_z^2}{2\mu^2}-\epsilon(\nu^2+\mu^2)$$
$$+\frac{1}{8}\nu^2\mu^2(\nu^2+\mu^2)\equiv 2 \tag{29}$$

at the fixed pseudoenergy 2. For negative scaled energies $\epsilon<0$, i.e., compact phase space, the Hamiltonian (29) represents a sextic oscillator: Two harmonic oscillators with frequency $\omega=\sqrt{-2\epsilon}$, which are coupled by the term $\nu^2\mu^2(\nu^2+\mu^2)$ due to the diamagnetic interaction. The trajectories generated by the Hamiltonian $H$ and $h$ are not related by a canonical transformation, but there is a one-to-one correspondence. In the following we confine ourselves to vanishing angular momentum $l_z=0$ and use a scaled energy $\epsilon=-0.1$ for which the classical atom is almost completely chaotic. Although the SD method works also in systems with considerable fractions of the phase space being integrable, we concentrate on the situation of almost fully chaotic phase space.

The equations of motion in the semi parabolic coordinates are derived in a straightforward way from the Hamiltonian (29):

$$\dot{\mu} = \frac{\partial h}{\partial p_\mu} = p_\mu, \tag{30}$$

$$\dot{\nu} = \frac{\partial h}{\partial p_\nu} = p_\nu, \tag{31}$$

$$\dot{p}_\mu = -\frac{\partial h}{\partial \mu} = \epsilon\mu - \frac{1}{4}\mu\nu^4 - \frac{1}{2}\mu^3\nu^2, \tag{32}$$

$$\dot{p}_\nu = -\frac{\partial h}{\partial \nu} = \epsilon\nu - \frac{1}{4}\nu\mu^4 - \frac{1}{2}\nu^3\mu^2. \tag{33}$$

These equations of motion are integrated using a Taylor–integration scheme [42] (due to energy conservation the dynamics takes place on a three-dimensional energy shell). This algorithm is best suited to integrate Hamiltonian of polynomial structure. The temporal derivatives of the phase space coordinates are expanded in a Taylor series up to a given order *N*. Hereby we make extensive use of the corresponding recursion relations. The stability matrix can be expanded and integrated the same way (for details see Ref. [42]). This Taylor integrator is an extremely powerful tool to reliably integrate the equations of motion (an optimal order to be used is typically $N=18$).

The PSS is given by the hyperplane

$$\{\nu, p_\nu, \mu = 0\} \tag{34}$$

Due to the exchange symmetry $\mu \leftrightarrow \nu$ of the Hamiltonian Eq. (29) and the equations of motion (30)–(33) this choice of the PSS gives the same numerical values of the position of the UPOs as the choice $\{\mu, p_\mu, \nu = 0\}$. The position of a point in the PSS is therefore given by the pair of coordinates $(\nu, p_\nu)$. Using a bisection method the latter is determined within an accuracy of $|\mu| < 10^{-15}$. The intersection of the three-dimensional energy surface with the PSS defines a two-dimensional area in this surface in which the dynamics of the system takes place. Equation (29) with $p_\mu^2 \geqslant 0$ shows that the area in the PSS allowed for the dynamics is given by

$$p_\nu^2 - 2\epsilon\nu^2 \leqslant 4 \tag{35}$$

i.e., in coordinates $(\sqrt{-2\epsilon}\nu, p_\nu)$ this area is given by a circle of radius 2. The Hamiltonian Eq. (29) with $l_z = 0$ and $\mu = 0$ defines the initial value $p_\mu = 2\sqrt{2 - \epsilon\nu^2 - \frac{1}{2}p_\nu^2}$ corresponding to an initial point $(\nu, p_\nu)$ in the surface of section. It is sufficient to consider just one sign (+ in this case) for the square root on the right-hand side since there are always symmetric pairs of orbits related by reflection at the PSS.

The role of the number of intersections of an UPO is different when compared to the Lorenz system. Now we encounter also long UPOs possessing only a few intersections of the PSS as well as relatively short ones that intersect the PSS quite often. Therefore it is possible to find extremely long orbits as fixed points of the only a few times iterated

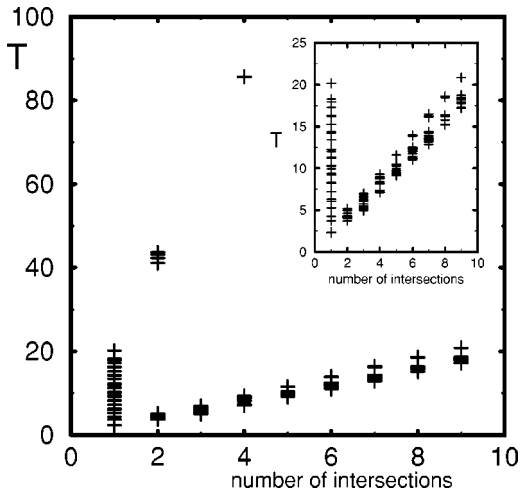


FIG. 6. The hydrogen atom in magnetic field: Distribution of the length of the periodic orbits versus the number of their intersections in the PSS. The inset shows the low-period part of the distribution.

Poincaré map. Figure 6 shows the distribution of the length of the UPOs. A particular example of such an orbit is illustrated in Fig. 7. To find UPOs with just one or two intersections we took a large number of initial conditions (typically several thousand) and found several long orbits as the one shown in Fig. 7. The majority of the orbits, of course, are significantly shorter and have a simpler appearance. The increase of the length of their periods with the number of intersections is nearly linear (see Fig. 6, inset) similar to the Lorenz system. If the grid of initial points becomes larger and the parameter λ becomes smaller we can detect increasingly more and longer UPOs in a given area of the PSS. We used rather large grids of initial points for the detection of UPOs up to four intersections. For more intersection points a smaller grid of initial points has been applied. As a result we obtain large sets of UPOs possessing a significantly varying length, as visible in Fig. 6.

Using the SD method, one can control to some extent the topological features of the UPOs to be detected: Looking for UPOs starting with a large grid of initial points and a rather small value of the parameter λ one can detect long UPOs that linger for quite a time at a certain distance above and below the PSS [Fig. 8(a)]. The numerical effort herefore is

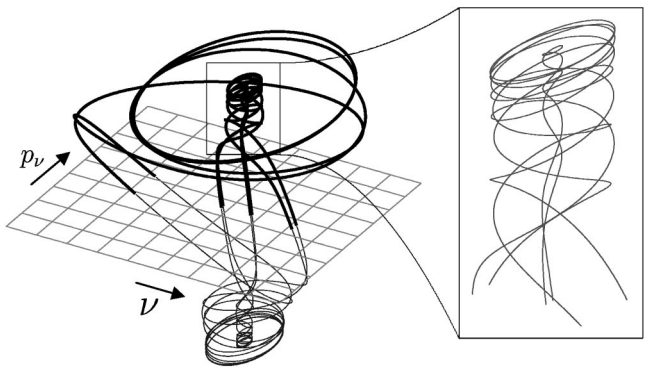


FIG. 7. Hydrogen atom in magnetic field: Example of a long periodic orbit with just four intersections with the PSS.

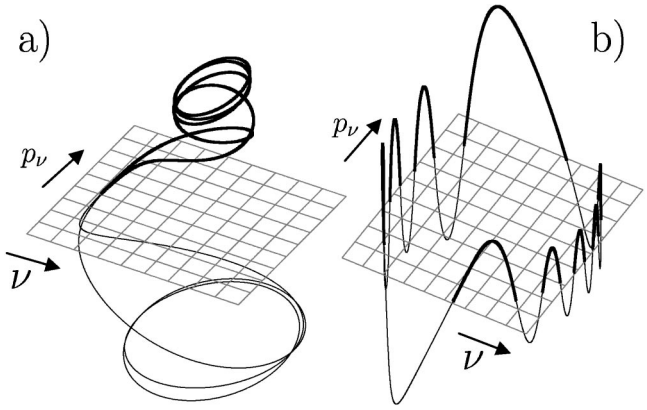


FIG. 8. Hydrogen atom in magnetic field: Periodic orbit with, a) a small number of intersections, located mainly above and below the PSS, b) a large number of intersections, located mainly in the PSS.

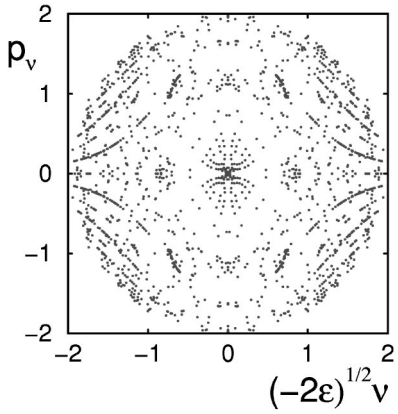


FIG. 9. Hydrogen atom in magnetic field: Location of periodic orbits with one up to nine intersections in the PSS.

minor, since for each step of the SD algorithm the Poincaré map has to be iterated just a few times. On the other side, looking for fixed points of the higher iterated Poincaré map, one might get, even for a relatively large $\lambda$, UPO's that have a crownlike appearance like in Fig. 8(b). The position of the PSS and the demanded number of intersections together with the parameter $\lambda$ and the set of starting points (see below) can therefore be used as a tool to determine, at least in a rough way, the topology of the UPOs to be found.

Determining the set of initial points is relatively straightforward for this system. The dynamics is supposed to be nearly ergodic, therefore a uniform random distribution of initial points in the surface of section is a good choice. The Hamiltonian Eq. (29) is symmetric with respect to the reflections $\nu \rightarrow -\nu$ and $p_\nu \rightarrow -p_\nu$. Therefore, each UPO with a given length appears four times in the total phase space, and the intersections with the PSS are located at coordinates related by the above symmetry operations. To avoid the convergence to UPOs that are trivially related by symmetry the initial points were distributed in a quarter segment of a circle with the coordinates $(\sqrt{-2\epsilon}\nu, p_\nu)$ and the radius 2.

Table II summarizes the result of our investigation. In contrast to the Lorenz system the minimal number of intersections is 1, corresponding to UPOs of the type given in Fig. 8(a). The number of UPOs with a given number of intersections and their mean length of period do not vary in a regular way as for the Lorenz system. The last row in Table II shows the minimal number $N_i$ of initial points that had to converge in order to find the listed number of UPOs. We used a set of 4000 initial points to detect UPOs up to four intersections. Since this number turned out to be larger than the necessary saturation $N_i$, we reduced it to 1000 initial points for UPOs with more than four intersections. However, again one has to keep in mind that not all initial points finally converge in an UPO. They might diverge or might not reach the desired accuracy within an appropriate time interval. In contrast to the Lorenz attractor, the propagation of each of the SD-transformed systems within the complete minimal set $\{\mathbf{S}_1, \mathbf{S}_3, \mathbf{S}_4\}$ yielded distinct orbits.

Figure 9 finally shows the intersection points of all UPOs given in Table II. To generate this figure the intersection points have been mirror imaged by the $\sqrt{-2\epsilon}\nu$ and $p_\nu$ axes. The dynamics is supposed to be ergodic, i.e., a chaotic trajectory fills the intersection of the energy surface and the PSS with uniform density. Nevertheless, the pattern of the intersections of the UPOs suggest some reminiscent structure in phase space. Especially for larger absolute values of $\sqrt{-2\epsilon}\nu$ a shell-like structure emerges. Given a value of $|\sqrt{-2\epsilon}\nu|$, certain values of $|p_\nu|$ seem to be favored by UPOs. With $|\sqrt{-2\epsilon}\nu|$ approaching its maximal value of 2, these favored values continuously decrease to zero.

## VI. SUMMARY AND OUTLOOK

We demonstrated that the SD method for chaotic time-discrete dynamical systems is easy to implement and at the same time a very efficient algorithm for the detection of (unstable) periodic orbits of continuous-time differential equations. The basic idea is the reduction of the continuous flow of the system to a discrete Poincaré map. The Poincaré map is then scanned for periodic points, i.e., fixed points of the iterated map. This way, the transformations that stabilize the

TABLE II. Hydrogen atom in magnetic field. Properties of periodic orbits with one up to nine intersections with the PSS, and parameters of the numerical detection: The parameter $\lambda$ and the required number of converged initial points $N_i$, sampled from the attractor.

| Number of intersections | 1 | 2 | 3 | 4 | 5 | 6 | 7 | 8 | 9 |
|---|---|---|---|---|---|---|---|---|---|
| Number of prime orbits | 29 | 14 | 16 | 13 | 12 | 19 | 19 | 11 | 11 |
| Mean period | 10.814 | 15.248 | 6.055 | 14.333 | 9.955 | 12.320 | 14.519 | 17.083 | 18.554 |
| $\lambda$ | 0.005 | 0.005 | 0.005 | 0.005 | 0.001 | 0.001 | 0.001 | 0.001 | 0.0005 |
| $N_i$ | 482 | 1348 | 462 | 48 | 173 | 209 | 650 | 432 | 126 |

original chaotic system operate in the hyperplane of the section. This approach to time-continuous systems possesses all the advantageous features of the SD method: A large extension of the basins of attraction (which is of even greater importance in higher-dimensional time-continuous systems), a nearly monotonous relation of the discretization parameter $\lambda$ with the stability of the detected periodic orbits, and a correlation of the geometrical features of the detected periodic orbits and the particular form of the corresponding stabilizing transformation. Moreover, the freedom to choose the PSS can be used to selectively detect periodic orbits possessing a certain topological structure. The two systems investigated here have a three-dimensional phase space. However, continuation of the method to higher dimensions provides no principal obstacles and will be limited by computational resources only. As demonstrated with the example of the Lorenz system there might be even less than the minimal set of SD transformations necessary to find all periodic orbits. It is expected that the convergence is even faster in higher-dimensional systems. Compared to methods that require the starting point to be close to the periodic orbit (like the Newton algorithm) the SD algorithm is expected to perform significantly better and offers a variety of possibilities to selectively investigate dynamical systems without prior knowledge on them.

## ACKNOWLEDGMENTS

The authors thank the Deutsche Forschungsgesellschaft and the Landesgraduiertenförderung Baden-Württemberg (D.P.) for financial support. Financial support in the framework of the IKYDA program of the DAAD (Germany) and IKY (Greece) is gratefully acknowledged. We thank J.Main for valuable discussions. The hospitality of the Department of Physics (D.P. and P.S.) of the University of Athens is also appreciated.

[1] M. C. Gutzwiller, *Chaos in Classical and Quantum Mechanics* (Springer-Verlag, New York, 1990).
[2] M. Brack and R.K. Bhaduri, *Semiclassical Physics*, Frontiers in Physics (Addison Wesley, New York, 1997).
[3] *Classical, Semiclassical and Quantum Dynamics in Atoms*, edited by H. Friedrich and B. Eckhardt, Lecture Notes in Physics **485** (Springer, Berlin, 1997).
[4] R. Artuso, E. Aurell, and P. Cvitanović, Nonlinearity **3**, 325 (1990).
[5] R. Artuso, E. Aurell, and P. Cvitanović, Nonlinearity **3**, 361 (1990).
[6] P. Cvitanović *et al.*, *Classical and Quantum Chaos* Web book http://www.nbi.dk/ChaosBook/Welcome.html
[7] C. Grebogi, E. Ott, and J. A. Yorke, Phys. Rev. A **37**, 1711 (1988).
[8] P. Cvitanović, G. H. Gunaratne, and I. Procaccia, Phys. Rev. A **38**, 1503 (1988).
[9] I. B. Schwartz and I. Triandaf, Phys. Rev. A **46**, 7439 (1992).
[10] H. D. I. Abarbanel, R. Brown, J. J. Sidorowich, and L. Sh. Tsimring, Rev. Mod. Phys. **65**, 1331 (1993).
[11] R. Badii, E. Brun, M. Finardi, L. Flepp, R. Holzner, J. Parisi, C. Reyl, and J. Simonet, Rev. Mod. Phys. **66**, 1389 (1994).
[12] P. So, E. Ott, S. J. Schiff, D. T. Kaplan, T. Sauer, and C. Grebogi, Phys. Rev. Lett. **76**, 4705 (1996).
[13] P. Grassberger, H. Kantz, and U. Moenig, J. Phys. A **22**, 5217 (1989).
[14] O. Biham and M. Kvale, Phys. Rev. A **46**, 6334 (1992).
[15] P. Cvitanović, Phys. Rev. Lett. **61**, 2729 (1988).
[16] E. Ott, *Chaos in Dynamical Systems* (Cambridge University Press, Cambridge, 1993).
[17] K. T. Hansen, Phys. Rev. E **52**, 2388 (1995).
[18] S. M. Zoldi and H. S. Greenside, Phys. Rev. E **57**, R2511 (1998).
[19] O. Biham and W. Wenzel, Phys. Rev. Lett. **63**, 819 (1989).
[20] M. Hénon, Commun. Math. Phys. **50**, 69 (1976).
[21] O. Biham and W. Wenzel, Phys. Rev. A **42**, 4639 (1990).
[22] W. Wenzel, O. Biham, and C. Jayaprakash, Phys. Rev. A **43**, 6550 (1991).
[23] P. Schmelcher and F. K. Diakonos, Phys. Rev. Lett. **78**, 4733 (1997).
[24] P. Schmelcher and F. K. Diakonos, Phys. Rev. E **57**, 2739 (1998).
[25] D. Pingel, P. Schmelcher, F. K. Diakonos, and O. Biham, Phys. Rev. E **62**, 2119 (2000).
[26] F. K. Diakonos, P. Schmelcher, and O. Biham, Phys. Rev. Lett. **81**, 4349 (1998).
[27] K. Ikeda, Opt. Commun. **30**, 257 (1979); S. M. Hammel, C. K. R. T. Jones, and J. V. Moloney, J. Opt. Soc. Am. B **4**, 552 (1985).
[28] F. K. Diakonos, D. Pingel, and P. Schmelcher, Phys. Rev. E **62**, 4413 (2000).
[29] Y. L. Bolotin, V. Y. Gonchar, A. A. Krokhin, A. Tur, and V. V. Yanovsky, Phys. Rev. Lett. **82**, 2504 (1999).
[30] R. L. Davidchack, Y. C. Lai, E. M. Bollt, and M. Dhamala, Phys. Rev. E **61**, 1353 (2000).
[31] Y. C. Lai, Phys. Rev. E **59**, 3807 (1999).
[32] R. L. Davidchack and Y.-C. Lai, Phys. Rev. E **60**, 6172 (1999).
[33] R. L. Davidchack, Y.-C.Lai, Aaron Klebanoff, and E. Bollt (unpublished).
[34] H. Ito, M. Murakita, I. Wakabayashi, A. Kumamoto, Conference Proceedings ECCTD'01 (2001) (unpublished).
[35] E. N. Lorenz, J. Atmos. Sci. **20**, 130 (1963).
[36] E. Kazentsev, Institut National de Recherche en Informatique et en Automatique, Rapport de Rechereche No. 3344, 1998 (unpublished).
[37] C. Sparrow, *The Lorenz Equations: Bifurcations, Chaos and Strange Attractors* (Springer, New York, 1982).
[38] H. Friedrich and D. Wintgen, Phys. Rep. **183**, 37 (1989).
[39] G. Tanner, K. T. Hansen, and J. Main, Nonlinearity **9**, 1641 (1996).
[40] D. Wintgen and A. Hönig, Phys. Rev. Lett. **63**, 1467 (1989).
[41] B. Eckhardt, C. Hose, and E. Pollak, Phys. Rev. A **39**, 3776 (1989).
[42] H. D. Meyer, J. Chem. Phys. **84**, 3147 (1986).